MAGNETISM
AND FERROELECTRICITY

Ferroelectric Phenomena in CdSnO₃: A First-Principles Studies

A. I. Lebedev

Moscow State University, Moscow, 119991 Russia
e-mail: swan@scon155.phys.msu.ru
Received December 1, 2008

Abstract—The phonon spectrum of cubic cadmium metastannate and parameters of the crystal structure of its distorted phases were calculated from first principles within the density functional theory. It is shown that the phonon spectrum and the energy spectrum of the distorted phases in α-CdSnO$_3$ resemble surprisingly the corresponding characteristics of CdTiO$_3$. The ground state of α-CdSnO$_3$ is the ferroelectric $Pbn2_1$ phase, the energy gain from the phase transition to this phase from the nonpolar phase $Pbnm$ is ~30 meV, and the spontaneous polarization is 0.25 C/m^2. The analysis of the eigenvector of the ferroelectric mode in α-CdSnO$_3$ and the partial densities of states indicates that the ferroelectric instability in this crystal, which does not contain transition d-element atoms, is associated with the formation of a covalent bonding between Cd and O atoms.

1. INTRODUCTION

Among a large family of ferroelectrics with the perovskite structure ABO$_3$, crystals in which A is the cadmium atom are least studied. In the CdO−SnO$_2$ system, two compounds are formed: CdSnO$_3$ and Cd$_2$SnO$_4$ [1]. Cadmium metastannate CdSnO$_3$ exists in two stable modifications: with an orthorhombically distorted perovskite structure (α-modification) [1−3] and with the rhombohedral ilmenite structure (β-modification) [3, 4]. As in the case of cadmium titanate, CdSnO$_3$ crystals with the ilmenite structure are obtained at a synthesis temperature of $\leq$800°C [5, 6] and crystals with the perovskite structure, at a temperature of 1000−1100°C [1, 5] or at high pressures [3]. Besides, upon decomposition of CdSn(OH)$_6$ it is possible to obtain CdSnO$_3$ with a metastable spinel structure [7]. Cadmium orthostannate (Cd$_2$SnO$_4$) also exists in two crystal modifications: with the orthorhombic Sr$_2$PbO$_4$ structure and with the spinel structure [7]. All these compounds are n-type semiconductors with a band gap of 2−3 eV [8, 9], which, due to a high concentration of native defects, are characterized by a rather high conductivity ($\sigma = 10^{-5}$−5 × 10^3 Ω^{-1} cm^{-1}). The latter circumstance hampers the study of these materials by dielectric methods. Cadmium stannates are used for fabrication of conducting thin film transparent to visible light and as gas sensors.

Cadmium metastannate with the perovskite structure is of interest as a potential ferroelectric. Unfortunately, there have been few studies of this material. The α-CdSnO$_3$ crystal structure was studied at a temperature of 300 K for powders [1] and single crystals [3] and identified as a structure with $Pbnm$ space group. A refined analysis of X-ray reflection intensities [10] suggested the possibility of polar state of this phase (the proposed space group $Pbn2_1$). The same conclusion was made by the authors of [11]. The analysis of the optical absorption and luminescence spectra [9] revealed, in the temperature dependence of the band gap $E_g(T)$ for α-CdSnO$_3$ single crystals, a region of rapid change in E_g (by 0.11 eV) at $T \approx 80$°C and two more regions of change near 140 and 200°C, which were associated with phase transitions in the crystals. In these temperature ranges, drastic changes in the intensity of luminescence and degree of its polarization were also observed. If these peculiarities are really due to the ferroelectric phase transition, we deal with a rare case when the ferroelectric properties appear in perovskite crystals, which do not contain transition d-elements.

The objective difficulties of studying cadmium metastannate, incompleteness of experimental data in literature, and the lack of understanding of the nature of ferroelectricity, which is proposed in this compound, make it expedient to calculate the physical properties of α-CdSnO$_3$ from first principles.

2. CALCULATION TECHNIQUE

The calculations were performed within the density functional theory using the pseudopotentials and plane-wave expansion of wave functions as implemented in the ABINIT code [12]. The exchange-correlation interaction was described in the local density approximation (LDA) following [13]. The pseudopotentials used were optimized separable nonlocal pseudopotentials [14] constructed using the OPIUM software package; the local potential [15] was added to them to improve their transferability. The parameters used for constructing the pseudopotentials, the results
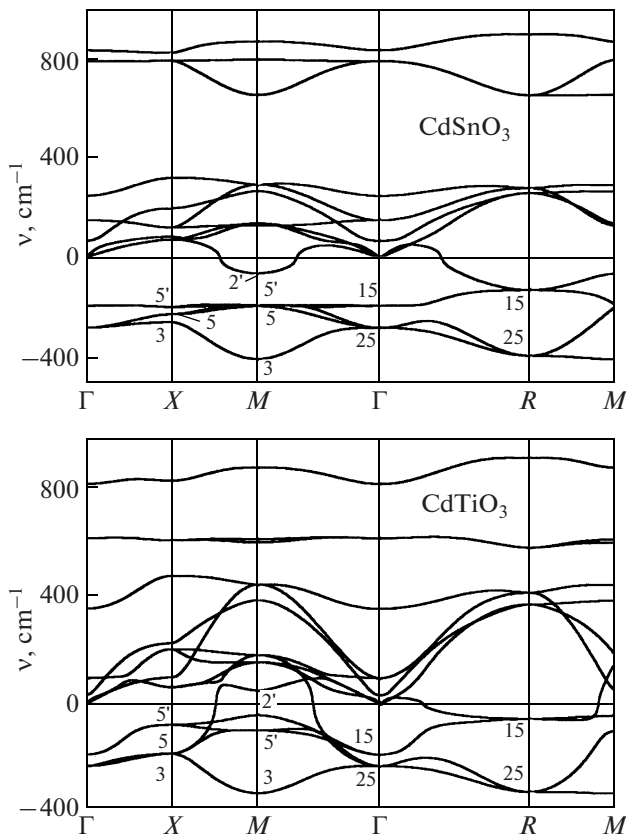
Fig. 1. Comparison of the phonon spectrum for the cubic parent phase of $CdSnO_3$ with the phonon spectrum of the same phase for $CdTiO_3$ [16]. Labels near the curves indicate the symmetry of the modes.

of testing the pseudopotentials, and other details of calculations are presented in [16].

3. RESULTS OF THE CALCULATIONS

3.1. Comparison of the Properties of $CdSnO_3$ and $CdTiO_3$

Figure 1 shows the phonon spectra of α-$CdSnO_3$ and $CdTiO_3$ crystals in the cubic parent phase with the perovskite structure. The comparison of these spectra reveals their surprising resemblance. This enables one to suppose that other physical properties of these crystals are similar as well.

Table 1 presents the energies of different low-symmetry phases formed in distortion of the cubic parent phase of cadmium metastannate according to the eigenvectors of unstable phonons that are present in its phonon spectrum. For comparison, the results of previous calculations of the energy of distorted phases in cadmium titanate [16, 17] are included in the table. The existence of one more unstable M_5 mode in $CdSnO_3$ corresponding to a distortion of the structure with rotation of octahedra leads to two more low-symmetry phases with space groups *Cmma* and *Pmna*. It is

evident that the energy spectra of different distorted phases in α-$CdSnO_3$ and $CdTiO_3$ are very similar, which confirms the similarity of these crystals. The nonpolar phase in cadmium metastannate with the lowest energy is the orthorhombic *Pbnm* phase.

Table 2 presents the calculated structural parameters for the *Pbnm* phase of cadmium metastannate. As follows from comparison with the data in literature, the calculated lattice parameters are close to the experimentally observed ones. A slight overestimate of the calculated lattice parameters is due to the peculiarity of the pseudopotential for a tin atom, which manifests itself in the tests as the overestimated lattice parameters of SnO_2 and gray tin. The atomic coordinates in the unit cell agree well with the results of the structure determination of α-$CdSnO_3$ [18], which was performed under the assumption that the space group of the crystal is *Pbnm*.

Simultaneously with calculating the structure of α-$CdSnO_3$, the structure of β-$CdSnO_3$ (space group $R\bar{3}$) was calculated. The calculated lattice parameters of this phase ($a = 5.5238$ Å, $c = 14.6550$ Å) were found to be close to those obtained experimentally ($a = 5.4530$ Å, $c = 14.960$ Å [3]). The energy gain of the $R\bar{3}$ phase of cadmium metastannate was by 77 meV lower than that of the $Pbn2_1$ phase. This means that, at $T = 0$, the phase with the structure of distorted perovskite is metastable. It should be noted that according to our data, in $CdTiO_3$, which also exists in ilmenite and perovskite modifications, the energy of the $R\bar{3}$ phase at $T = 0$ is by 166 meV lower than that of the *Pbnm* phase. The difference in the entropy contributions to the thermodynamic potential Φ can result in intersection of the curves for $\Phi(T)$ for the two considered phases. This can explain why one obtains crystals with the ilmenite structure at a low synthesis temperature and crystals with the perovskite structure at a high synthesis temperature (see Section 1).

3.2. Ferroelectric Phase in $CdSnO_3$

In order to verify the possible existence of the polar state in α-$CdSnO_3$, the frequencies of phonons at the Γ point were calculated for the orthorhombic *Pbnm* phase of this crystal. The calculations revealed one unstable optical mode of symmetry B_{1u} with a frequency of $89i$ cm^{-1}, which can be associated with the ferroelectric phase transition *Pbnm* $\longrightarrow$ *Pnb2_1*.

The calculated equilibrium atomic positions and lattice parameters for the $Pbn2_1$ phase are presented in Table 2. The lattice distortion is accompanied by a noticeable rearrangement of the local environment of the Cd atom; it results in that the average distance to four nearest oxygen atoms increases by 0.017 Å but another two oxygen atoms become closer by 0.23 Å. Thus, the ferroelectric lattice distortion is accompanied by an increase in the effective coordination num-

Table 1. Comparison of the relative energies of different low-symmetry phases of $CdTiO_3$ and $CdSnO_3$ (the energy of the cubic phase was taken as the energy origin)

CdTiO₃ [16, 17]			CdSnO₃		
unstable mode	space group	energy, meV	unstable mode	space group	energy, meV
R_{15}	$I4/mmm$	−24	M_5	$Cmma$	−141
X_3	$P4_2/mmc$	−45	M_5	$Pmna$	−262
Γ_{25}	$P\bar{4}m2$	−134	X_3	$P4_2/mmc$	−404
X_5	$Pmma$	−160	X_5	$Pmma$	−474
Γ_{15}	$R3m$	−245	R_{15}	$I4/mmm$	−536
X_5	$Cmcm$	−282	Γ_{25}	$P\bar{4}m2$	−540
Γ_{15}	$P4mm$	−340	Γ_{15}	$R3m$	−753
Γ_{15}, Γ_{25}	$Amm2$	−412	X_5	$Cmcm$	−886
Γ_{25}	$R32$	−486	Γ_{15}	$P4mm$	−1079
R_{25}	$I4/mcm$	−912	Γ_{15}, Γ_{25}	$Amm2$	−1259
M_3	$P4/mbm$	−920	Γ_{25}	$R32$	−1450
R_{25}	$R\bar{3}c$	−1197	M_3	$P4/mbm$	−1617
R_{15}	$C2/m$	−1202	R_{25}	$I4/mcm$	−1659
$R_{25} + M_3$	$Pbnm$	−1283	R_{15}	$C2/m$	−2455
B_{2u}	$Pb2_1m$	−1285	R_{25}	$R\bar{3}c$	−2460
B_{1u}	$Pbn2_1$	**−1290**	$R_{25} + M_3$	$Pbnm$	−2575
			B_{1u}	$Pbn2_1$	**−2605**

Note: The bold number is the energy of the ground state.

Table 2. Lattice parameters a, b, and c (in Å) and atomic coordinates in $CdSnO_3$ crystals with space groups $Pbnm$ and $Pbn2_1$

Parameter	This work		Experiment			
	$Pbnm$	$Pbn2_1$	[1]	[3]	[11]	[18]*
a	5.5024	5.5284	5.547	5.4578	5.4593	5.4588
b	5.5982	5.5972	5.577	5.5773	5.5804	5.5752
c	7.9770	7.9584	7.867	7.8741	7.8771	7.8711
Cd_x	−0.00861	−0.00553				−0.0092
Cd_y	+0.04816	+0.03818				+0.0423
Cd_z	+0.25000	+0.26021				+0.2500
Sn_x	+0.00000	+0.00036				+0.0000
Sn_y	+0.50000	+0.51455				+0.5000
Sn_z	+0.00000	−0.00209				+0.0000
$O1_x$	+0.12498	+0.12340				+0.114
$O1_y$	+0.42809	+0.42802				+0.455
$O1_z$	+0.25000	+0.24122				+0.2500
$O2a_x$	+0.68331	+0.66193				+0.695
$O2a_y$	+0.31304	+0.35381				+0.301
$O2a_z$	+0.06830	+0.04275				+0.058
$O2b_x$	+0.31669	+0.29516				+0.305
$O2b_y$	+0.68696	+0.72657				+0.699
$O2b_z$	−0.06830	−0.09020				−0.058

* In the structure determination, the space group was assumed to be $Pbnm$.

Table 3. Eigenvectors ξ of the ferroelectric mode B_{1u} and effective atomic charges Z^* in $CdSnO_3$ and $CdTiO_3$ crystals with space group *Pbnm* and in $BaTiO_3$ with space group *Pm3m*

Atom	ξ_x	ξ_y	ξ_z	Z^*_{xx}	Z^*_{yy}	Z^*_{zz}
Cd	+0.00000	+0.00000	+0.18913	+2.462	+2.506	+2.440
Sn	+0.00257	+0.12515	−0.01935	+4.379	+4.407	+4.338
O1	+0.00000	+0.00000	−0.05940	−2.052	−1.894	−2.905
O2	−0.13111	+0.20564	−0.19455	−2.395	−2.509	−1.937
Cd	+0.00000	+0.00000	+0.10628	+2.570	+2.500	+2.592
Ti	+0.01863	−0.19067	+0.15463	+7.363	+7.693	+7.260
O1	+0.00000	+0.00000	−0.16286	−2.194	−1.957	−5.650
O2	−0.07161	+0.18255	−0.19322	−3.869	−4.118	−2.101
Ba			+0.02988			+2.738
Ti			+0.67340			+7.761
O1			−0.54043			−6.128
O2			−0.35607			−2.186

ber of the Cd atom. The energy gain from the phase transition *Pbnm* $\longrightarrow$ *Pbn*2_1 is $\Delta E = 30.5$ meV (Table 1). The sufficiently large energy gain allows one to expect that the structure will be ferroelectric at room temper-

Fig. 2. Partial contributions of the *s*, *p*, and *d* states of the Cd, Sn, O1, and O2 atoms to the density of states in the orthorhombic phase *Pbnm* of $CdSnO_3$. The energy origin is taken at the top of the valence band.

ature in agreement with the data of [10, 11]. Indeed, the phase transition temperature ($\Delta E/k \sim 350$ K) estimated from the energy gain from the transition to the ferroelectric phase is found to be close to the temperature of 80°C, at which the most drastic changes in the absorption spectra were observed [9]. The calculation of the spontaneous polarization in $CdSnO_3$ with *Pbn*2_1 m structure using the Berry-phase method [19] gives an unexpectedly high value of $P_s = 0.25$ C/m^2, which is close to spontaneous polarization in barium titanate.
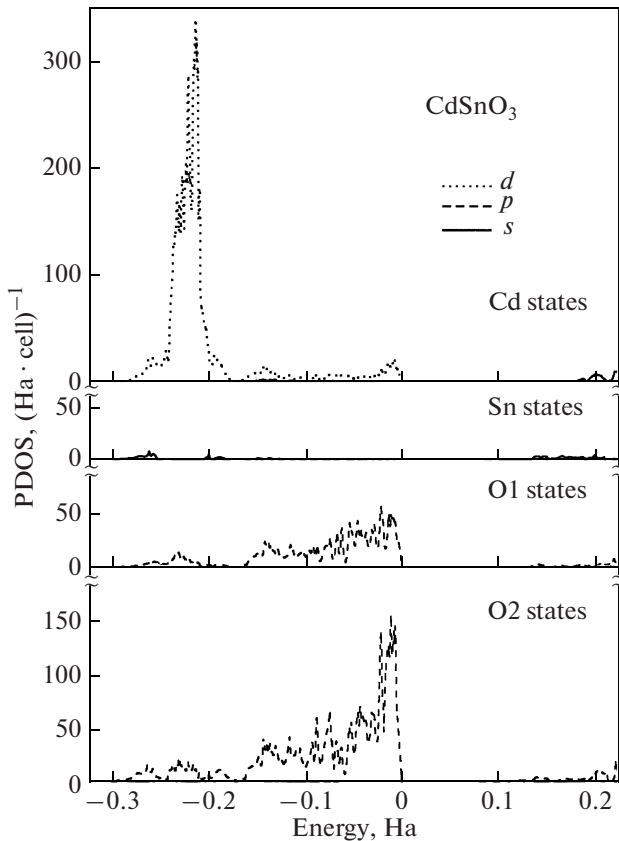
4. DISCUSSION OF THE RESULTS

The results of our calculations show that the ferroelectricity can appear in perovskite crystals that do not contain the atoms of transition *d*-elements. Let us try to understand the nature of such phase transitions.

The appearance of the ferroelectric phase transition in α-$CdSnO_3$ cannot be associated with an off-center position of cadmium atoms. Although, in the cubic parent phase of $CdSnO_3$, the diagonal element of the on-site force constant matrix for Cd atoms is −0.0111 Ha/Bohr^2, which indicates its off-center position, in the *Pbnm* phase, after the unit cell volume decreased by 8.4%, the minimum value of the diagonal element increases to +0.0714 Ha/Bohr^2 and the potential well for the Cd atom becomes on-center.[1]

Now, we consider the characteristics of the ferroelectric soft mode. Table 3 presents the eigenvectors ξ of the dynamic matrix for the B_{1u} mode in α-$CdSnO_3$ and $CdTiO_3$ crystals and, for comparison, the Γ_{15} mode in $BaTiO_3$. Here, O1 denotes oxygen atoms forming, with *B* atoms, chains that go in the direction of the polar axis of the ferroelectric phase and O2

---

[1] In the present work, the values of the force constant matrix and the partial densities of states are given in the Hartree system of atomic units.

denotes the remaining oxygen atoms. The analysis of the eigenvector of the B_{1u} mode in α-CdSnO$_3$ shows that the main contribution to the ferroelectric mode is made by Cd and O2 atoms. At the same time, the Sn atom substantially shifts only in the y direction perpendicular to the polar axis and its small shift along the polar axis takes place in the opposite phase with cadmium atoms and in phase with oxygen atoms. This means that the main role in the appearance of ferroelectricity in α-CdSnO$_3$ is played by cadmium atoms. The comparison of eigenvectors of ferroelectric modes in these three crystals reveals that cadmium metastannate and barium titanate are the limiting cases, in which the appearance of ferroelectricity is caused by A and B atoms in the perovskite structure ABO$_3$, and cadmium titanate is an intermediate case.

The effective atomic charges Z^* in the $Pbnm$ phase of cadmium metastannate (Table 3) are close to formal valences of atoms. In the cubic parent phase, the charge for Sn atoms is slightly smaller

than that in the orthorhombic phase ($Z^* = 4.17$) and, for Cd atoms, it is slightly greater ($Z^* = 3.26$).

For better understanding of the nature of ferroelectric instability and of the character of chemical bonding in α-CdSnO$_3$, the partial densities of states (contributions of s, p, and d orbitals of Cd, Sn, O1, and O2 atoms to the total density of states) were calculated. The results of these calculations are presented in Fig. 2. As follows from the figure, the overlap of Cd $4d$ states and O $2p$ states plays an important role in the formation of chemical bonding in the crystal; comparable contributions from these states give evidence for a noticeable covalent component in this bonding. The contribution of Sn $5s$ and Sn $5p$ states to the valence band is much smaller than that of Cd atoms, which suggests a predominantly ionic character of the Sn–O bonds. The Sn $5s$ states overlapping with O $2p$ states make the main contribution to the conduction band ($E > 0.037$ Ha in Fig. 2). It should be noted that, although the partial densities of states for α-CdSnO$_3$ were already calculated in [18], that work did not analyze the role of Cd $4d$ states, whose contribution to the density of states, according to our calculations, is several times greater than the contribution of Sn $5s$ states. The conclusion of an important role of covalent interaction between Cd and O atoms, which follows from the analysis of partial densities of states, agrees with the results given by the analysis of the eigenvector of the ferroelectric mode and suggests that the rearrangement of these bonds is the cause of the ferroelectric instability in α-CdSnO$_3$.

Table 4 presents calculated frequencies of the modes active in Raman and infrared (IR) spectra for crystals of CdSnO$_3$ with space groups $Pbnm$ and $Pbn2_1$. In the crystal with the $Pbnm$ structure, there are 24 Raman-active modes (modes with A_g, B_{1g}, B_{2g}, and B_{3g} symmetry) and 25 IR-active modes (modes with B_{1u}, B_{2u}, and B_{3u} symmetry). When the symmetry of crystals is lowered to $Pbn2_1$, all 57 optical modes

Table 4. Calculated frequencies of the IR- and Raman-active optical modes ν_i for CdSnO$_3$ crystals with space groups $Pbnm$ and $Pbn2_1$

Space group	Mode	ν_i, cm^{-1}
$Pbnm$	A_g	79, 130, 196, 290, 413, 452, 522
	B_{1g}	108, 150, 232, 347, 440, 500, 671
	B_{2g}	87, 207, 446, 474, 668
	B_{3g}	107, 142, 375, 500, 590
	B_{1u}	89i, 118, 163, 237, 390, 551, 594
	B_{2u}	62, 150, 175, 226, 264, 302, 420, 512, 605
	B_{3u}	90, 131, 186, 216, 267, 362, 420, 476, 640
$Pbn2_1$	A_1	78, 117, 138, 144, 201, 213, 241, 271, 375, 413, 436, 504, 562, 574
	A_2	93, 105, 121, 130, 149, 202, 226, 263, 351, 396, 432, 486, 539, 599, 655
	B_1	90, 120, 152, 206, 236, 251, 273, 351, 396, 443, 466, 483, 610, 658
	B_2	88, 131, 151, 193, 208, 238, 261, 298, 364, 421, 462, 515, 579, 603

become active in the Raman spectra and 42 modes of A_1, B_1, and B_2 symmetry become active in the IR spectra. Unfortunately, the IR-absorption spectra in the range 250–800 cm^{-1} for α-CdSnO$_3$ [20] available in literature consist of five very wide bands and their identification failed.

As for the prospects of further studies of ferroelectric properties of α-CdSnO$_3$, we should note the following. As was noted in Section 1, these crystals are n-type semiconductors and their temperature dependence of conductivity has a thermoactive character with an activation energy of 0.3 eV [3]. Therefore, if the hopping conductivity is not high, studies at low temperatures are possible. Donor levels supplying electrons to the conduction band are usually associated with the oxygen vacancies. However, a rather small effect of variations in the partial pressure of O$_2$ during annealing on the conductivity of α-CdSnO$_3$ [8] makes this explanation very unlikely. In [21], in the discussion of the properties of Cd$_2$SnO$_4$, the energy position of various defects was calculated and it was shown that the most important defect in this crystal is the antisite defect Cd$_{Sn}$. Perhaps, the same defects can determine the electrical conductivity of α-CdSnO$_3$. We hope that improvements in the technology of the crystal growth and doping of them with acceptors will make it possible in the future to obtain high-resistivity crystals of α-CdSnO$_3$, which will enable one to perform direct dielectric measurements.

5. CONCLUSIONS

The first-principles calculations confirm the existence of the stable ferroelectric phase $Pbn2_1$ in cad-

mium metastannate, the energy of which is 30.5 meV lower than the energy of the nonpolar phase *Pbnm*, and the spontaneous polarization is 0.25 C/m². The analysis of the eigenvector of the ferroelectric mode in α-CdSnO$_3$ and the partial densities of states shows that the ferroelectric instability in this crystal, which does not contain transition *d*-element atoms, is associated with the formation of the covalent bonding between Cd and O atoms.

ACKNOWLEDGMENTS

REFERENCES

1. A. J. Smith, Acta Crystallogr. **13**, 749 (1960).

2. I. Náray-Szabó, Naturwiss. **31**, 202 (1943).

3. R. D. Shannon, J. L. Gillson, and R. J. Bouchard, J. Phys. Chem. Solids **38**, 877 (1977).

4. I. Morgenstern-Badarau, P. Poix, and A. Michel, C. R. Acad. Sci., ser. IV **258**, 3036 (1964).

5. Z. Tianshu, S. Yusheng, D. Qiang, and F. Huajun, J. Mater. Sci. Lett. **13**, 1647 (1994).

6. Y.-L. Liu, Y. Xing, H.-F. Yang, Z.-M. Liu, Y. Yang, C.-L. Shen, and R.-Q. Yu, Anal. Chim. Acta **527**, 21 (2004).

7. *Landolt−Börnstein: Numerical Data and Functional Relationships in Science and Technology. New Series. Group III* (Springer, Berlin, 1986), Vol. 7d1g, p. 178.

8. F. Golestani-Fard, C. A. Hogarth, and D. N. Waters, J. Mater. Sci. Lett. **2**, 505 (1983).

9. E. N. Myasnikov, R. I. Spinko, E. A. Shalaeva, and T. P. Myasnikova, Ferroelectrics **214**, 177 (1998).

10. V. N. Lebedev, R. V. Kolesova, and E. G. Fesenko, in *Crystallization and Properties of Crystals* (Novocherkassk Polytechnical Institute, Novocherkassk, 1977), Issue 4, p. 96 [in Russian].

11. N. V. Prutsakova and Yu. V. Kabirov, Issled. Ross. (Élektron. Zh.) **7**, 2402 (2004); http://zhurnal.ape.relarn.ru/articles/2004/226.pdf.

12. X. Gonze, J.-M. Beuken, R. Caracas, F. Detraux, M. Fuchs, G.-M. Rignanese, L. Sindic, M. Verstraete, G. Zerah, F. Jollet, M. Torrent, A. Roy, M. Mikami, Ph. Ghosez, J.-Y. Raty, and D. C. Allan, Comput. Mater. Sci. **25**, 478 (2002).

13. J. P. Perdew and A. Zunger, Phys. Rev. B: Condens. Matter **23**, 5048 (1981).

14. A. M. Rappe, K. M. Rabe, E. Kaxiras, and J. D. Joannopoulos, Phys. Rev. B: Condens. Matter **41**, 1227 (1990).

15. N. J. Ramer and A. M. Rappe, Phys. Rev. B: Condens. Matter **59**, 12471 (1999).

16. A. I. Lebedev, Fiz. Tverd. Tela (St. Petersburg) **51** (2), 341 (2009) [Phys. Solid State **51** (2), 362 (2009)].

17. A. I. Lebedev, Fiz. Tverd. Tela (St. Petersburg) **51** (4), 757 (2009) [Phys. Solid State **51** (4), 802 (2009)].

18. H. Mizoguchi, H. W. Eng, and P. M. Woodward, Inorg. Chem. **43**, 1667 (2004).

19. N. Sai, K. M. Rabe, and D. Vanderbilt, Phys. Rev. B: Condens. Matter **66**, 104108 (2002).

20. I. L. Botto and E. J. Baran, Z. Anorg. Allg. Chem. **465**, 186 (1980).

21. S. B. Zhang and S.-H. Wei, Appl. Phys. Lett. **80**, 1376 (2002).

Translated by E. Chernokozhin